Vision Research 48 (2008) 1791–1797

Contents lists available at ScienceDirect

Vision Research

journal homepage: www.elsevier.com/locate/visres

Perceived roughness of $1/f^{\beta}$ noise surfaces

Stefano Padilla [a], Ondrej Drbohlav [c], Patrick R. Green [b,*], Andy Spence [a], Mike J. Chantler [a]

[a] School of Mathematical and Computer Sciences, Heriot-Watt University, Edinburgh, UK
[b] School of Life Sciences, Heriot-Watt University, Riccarton, Edinburgh EH14 4AS, UK
[c] Faculty of Computer and Information Science, University of Ljubljana, Slovenia

ARTICLE INFO

Article history:
Received 11 December 2007
Received in revised form 20 May 2008

Keywords:
Perceived roughness
Appearance
Roughness perception
Texture

ABSTRACT

We report results from a new methodology for investigating the visually perceived properties of surface textures. Densely sampled two-dimensional $1/f^{\beta}$ noise processes are used to model natural looking surfaces, which are rendered using combined point-source and ambient lighting. Surfaces are shown in motion to provide rich cues to their relief. They are generated in real time to enable observers to dynamically manipulate surface parameters. A method of adjustment is employed to investigate the effects that the two surface parameters, magnitude roll-off factor and RMS height, have on perceived roughness. The results are used to develop an estimation method for perceived roughness.

1. Introduction

The surfaces of most objects and materials vary in their relief (or surface height function), and in their reflectance. While these characteristics differ in detail from one patch of a surface to another, they have statistical properties that remain approximately constant and which define the surface texture. When a surface is illuminated and viewed, these properties are captured in the pattern of luminance and colour in its image, and define image texture. To the extent that effects of illumination on image texture can be resolved, an observer will be able to determine properties of surface texture. In turn, these provide information such as the large-scale slants and curvatures of surfaces (e.g. Malik & Rosenholtz, 1997; Saunders & Backus, 2006), or the physical properties, uses and identities of objects. In using texture to obtain such information about objects, we are able not only to recognise the surface textures characteristic of particular objects, but also to make judgements about the similarities and differences between surface textures. For example, we might use the surface texture of a novel fruit to help decide whether it belongs to a familiar edible category or not, or we might judge whether the surface textures of a wall covering and a fabric harmonise or not. In everyday language, we express our judgements of surface textures in terms of properties such as fineness, regularity or roughness, but can these perceived properties be identified with physical properties of surfaces?

Several methods have been used to determine the mappings between physical and perceived properties of surface textures. A number of studies have used sets of photographic images of a wide variety of natural or manufactured textured objects, such as those provided by the Brodatz album (Brodatz, 1966). In some cases (Amadasun & King, 1989; Tamura, Mori, & Yamawaki, 1978), observers were given predetermined texture properties and asked to rank the photographs according to how strongly they represented each one. The properties chosen were determined by proposed machine algorithms for measuring image textures, and correlations were found between human and machine rankings. However, not all the descriptive terms were ones that are used spontaneously in describing surfaces, and so the observers may have been implicitly prompted to look for texture properties corresponding to those which the algorithms were designed to measure. To overcome this problem, Heaps and Handel (1999), Long and Leow (2001), and Rao and Lohse (1996) used free sorting tasks, asking observers to sort photographs of textured surfaces into similar groups of their own choosing, without any prompts about the texture properties to use. Multidimensional scaling, cluster analysis and other methods were applied to the similarity matrices obtained in order to identify the dimensions that determined observers' judgements of similarity. However, there were differences between the studies in the number and the nature of the dimensions obtained, suggesting that this method does not identify stable perceived properties of textures. Heaps and Handel (1999) argued that an observer's similarity judgements are always influenced by the whole set of textures presented, and therefore that no context-free set of perceived dimensions exists.

Another approach to the problem of mapping physical and perceived properties of textures is to manipulate properties of images and to measure the effect on observers' perception of them. The difficulty with this approach lies in creating images that resemble images of real textured surfaces closely enough to engage the same

* Corresponding author. Fax: +44 131 451 3735.
E-mail address: P.R.Green@hw.ac.uk (P.R. Green).

0042-6989/$ - see front matter © 2008 Elsevier Ltd. All rights reserved.
doi:10.1016/j.visres.2008.05.015

perceptual mechanisms. Balas (2006) achieved this by using a texture synthesis algorithm (Portilla & Simoncelli, 2000) to create images that matched a sample photograph in a set of statistical properties. Observers then tried to detect the odd texture patch in triplets where one patch was from the original image and two were synthetic (or vice versa). The results identified which statistical properties were most critical for perceptually successful synthesis of particular types of texture. However, the experiments used brief (250 ms) stimulus presentations, and the results may not extend from pre-attentive vision to judgements made over longer periods of inspection.

The methods reviewed so far all share an important limitation. They work with single still images of textured surfaces, or synthetic images derived from them, and not with the surfaces themselves. Furthermore, these images have been obtained under arbitrary and unspecified illumination, and so will contain ambiguities about surface relief and reflectance which cannot be resolved, as in a natural situation, by altering the relative orientation of the surface and the illuminant (Belhumeur, Kriegman, & Yuille, 1999). One way of overcoming this problem is to use sets of photographs of a surface obtained under multiple, precisely controlled illumination conditions, such as the image database used by Koenderink, van Doorn, Kappers, te Pas, and Pont (2003) in experiments on observers' ability to judge the elevation and azimuth of a light source from images of textured surfaces. Another is to create models of surface relief and reflectance that are then rendered graphically under specified illumination. This second method has the advantages of speed and flexibility, although it depends on the quality of the model surface and its rendering. Ho and colleagues used this approach to investigate the stability of judgements of the roughness of a surface as the direction of illumination changed (Ho, Landy, & Maloney, 2006) or as the observer's viewpoint changed (Ho, Maloney, & Landy, 2007). They used surface models made up of irregular arrays of triangular facets, varying the mean height of the facets to create surfaces of different roughness. Observers were able to judge the relative roughness of images presented in pairs, but did not fully compensate for variation in the elevation of the light source, or in viewpoint. These results imply that roughness of these surfaces is judged by the use of approximate heuristics, or 'pseudocues', that support only partial roughness constancy.

In our experiments, we also present observers with images of synthetic surfaces (see Fig. 1 for examples), created by rendering a model of surface relief, and test the effects of varying specific parameters of the model on observers' judgements of surface roughness. However, these images are novel in two important respects. First, they have a more natural appearance, and are more densely sampled, than those used previously. Second, they are generated rapidly enough both to create animations simulating the rotation of a surface under a light source, and to allow observers to control surface parameters in real time.

We achieve a natural appearance by using isotropic surface models generated from $1/f^{\beta}$ noise, and rendered assuming Lambertian reflectance and a simple lighting model. By $1/f^{\beta}$ noise, we mean that the height map has a magnitude spectrum $H(f)$ scaled with spatial frequency, of the form:

$$H(f) = \frac{\sigma}{N(\beta)} f^{-\beta} \tag{1}$$

where β is the roll-off factor of the surface height magnitude spectrum (i.e. the inverse of its slope in log H and log f co-ordinates), σ is the RMS height of the surface and $N(\beta)$ is a normalising factor. A $1/f^{\beta}$ noise spectrum can be considered as a random fractal function generated in the frequency domain (Mandelbrot, 1983; Saupe, 1988). In our models, height maps are random-phase, and surfaces have uniform reflectance. The effects of varying two parameters of the height magnitude spectrum, the RMS height σ and the roll-off factor β are illustrated for examples of our surfaces in Fig. 1.

The surface model is rotated back and forth, creating a sequence of images of a surface that 'wobbles' under a fixed light source. Such a dynamic image sequence can provide observers with rich information about object structure, to resolve ambiguities existing in the case of single image stimuli (Belhumeur et al., 1999). Our dynamic stimuli can be thought of as simulating the way that humans commonly examine a real surface by turning it under a light.

To our knowledge, this technique for creating synthetic surfaces has not previously been used in research on texture perception. Harvey and Gervais (1981) controlled the spectral content of images used in a similarity judgement task by creating compound gratings made up of seven spatial frequencies with randomly chosen amplitudes, but these images did not have a natural appearance, and were not created by rendering surface models.

Our aim in these experiments is to define how observers' perception of the roughness of isotropic $1/f^{\beta}$ noise surfaces is determined by the parameters σ and β of the surface height magnitude spectrum. In Experiment 1, we use a method of adjust-

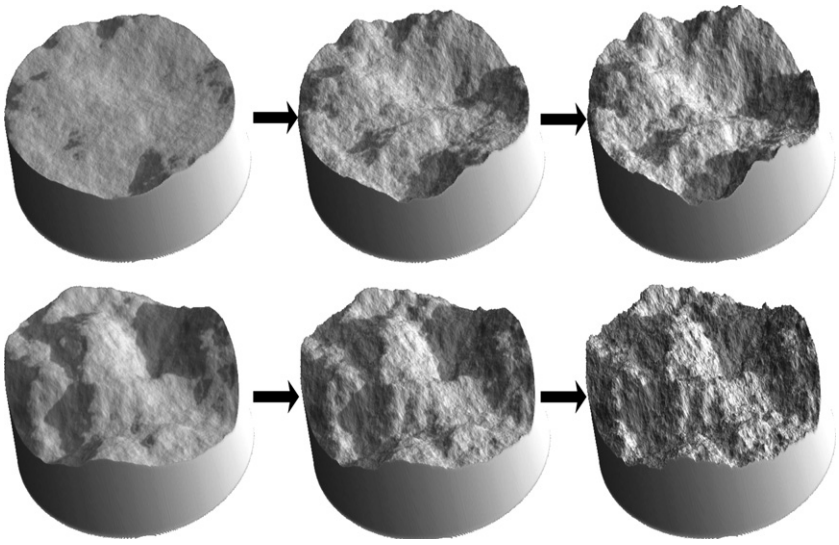

Fig. 1. (Top row, left to right) Surfaces with RMS height (σ) = 4, 8, and 12 mm. β = 2 in all three. (Bottom row, left to right) Surfaces with β = 2.2, 2.0, and 1.8. RMS height = 10 mm in all three.

ment to determine the combinations of these two parameters that give rise to equal perceived roughness. We then use these results to derive the parameters of an estimator of perceived roughness with the form of a bandpass filter. In Experiment 2, we use a bisection method (Fagot & Stewart, 1970) to determine how the output of the estimator is scaled with perceived roughness.

2. General methods

2.1. Observers

Data were obtained from a total of ten observers, all with normal or corrected-to-normal vision and naïve to the nature of the stimuli and the purpose of the experiments.

2.2. Stimuli

The surface models where generated in the frequency domain with randomphase and a controlled magnitude (β, σ). Two graphics cards (GeForce 7 series) were used for representing the surfaces; these were rendered using per-vertex displacement mapping to reduce approximation errors (Cook, 1984). For increased realism, per-pixel Lambertian shading with soft-edged cast shadow was applied in real time, but we did not implement interreflections. The lighting model was a point-light supplemented by an ambient 'fill' light with a luminance one third that of the point-light. The albedo of the surface was 0.6, corresponding to a natural material such as stone. The texture size chosen allowed us to match each pixel with its corresponding shading therefore avoiding aliasing artefacts. In total half a million faces were shaded (per-pixel) and displaced (per-vertex) in real time for each surface.

The surfaces were presented as the circular faces of cylindrical 'cakes', 130.5 mm (8.5 degrees of visual angle) in diameter (see Fig. 1). The sides of the stimuli were trimmed to avoid biasing observers with directionality, by superimposing a circular ramp around the surface relief. The stimuli were presented at a slant, with a mean angle of 32° between the macroscopic surface normal and a fronto-planar view, and were animated to simulate a repeated oscillation of the surface through 16° about this mean, with a period of approximately 2 s. The mean angle between the macroscopic surface normal and the light source was 60°. The animation used had been recorded during a pilot experiment in which observers were able to control surface motion while making a roughness judgement; this was the pattern of motion adopted by the observer who made the most consistent judgements. The values of viewing distance and stimulus diameter were chosen in order to present spatial frequencies between $f_1 = 0.117$ and $f_2 = 30$ cpd, covering most of the range to which the human visual system is sensitive (Campbell & Robson, 1968).

Pilot experiments indicated that observers were able to make consistent roughness judgements when values of the surface height magnitude spectrum roll-off factor β fell between 1.7 and 2.3, and this range of values was used in the experiments.

We presented the stimuli on two 20-in. TFT LCD monitors (NEC LCD2090UXi), with a pixel pitch of 0.255 mm (100 dpi). TFT monitors provide superior spatial modulation transfer functions to those of CRT models (Blume et al., 2003). We used panels with 12-bit look up tables for more accurate gamma correction, and of A-TW-IPS manufacture to increase viewing angle, colour reproduction, white colour balance, and increased gamut at a loss of response time (16 ms). A spectrophotometer (Gretag Macbeth Eye One Pro) was used to calibrate and equalise the linear gamma responses from both monitors, which produce a maximum error of 1.06 cd/m^2 (or 2.7%). In addition, to calibrate the maximum and minimum luminance was fixed to 100 and 0.7 cd/m^2, respectively. The variation in luminance across the area of the screen occupied by the stimuli was 5 cd/m^2. The observer's head was fixed using a chin rest so that the stimuli were at an optical distance of 88 cm. The monitors were rotated so that the observer's line of sight was approximately perpendicular to both screens at the centre of the stimuli.

3. Experiment 1

3.1. Procedure

The aim of experiment one was to measure how observers set one parameter (σ) of a surface in order to match its roughness to that of a surface that differs from it in the other parameter (β). On each trial, observers were presented with pairs of surfaces, one on each monitor screen, and instructed to match the two surfaces in roughness. In order to make it clear that the fine structures of the surfaces should be matched, rather than the large-scale structure of the 'cakes', they were also told to imagine how each surface would feel if touched. The parameters of one surface (the sample surface) were fixed during the trial, while moving the computer mouse altered in real time the RMS height (σ) of the other (the adjustable surface). Observers indicated by pressing the space bar when they thought both textures had similar roughness. No time limit was applied to observers' decisions, but they took on average 13 s to make matches. In the sample surface, β was always 2.0 and σ was one of five values (4–12 mm in 2 mm steps). In the adjustable surface, β had one of seven values (1.7–2.3 in steps of 0.1), and σ was under the observer's control, with a randomly chosen initial value. Following five practice trials, each of the 35 combinations of values was repeated three times, giving a total 110 trials, in a random order, for each of ten observers.

3.2. Results

Simple inspection of the synthetic textured surfaces shows that they appeared rougher with increasing RMS height σ and with decreasing β (see Fig. 1). The results of the experiment (see Fig. 2) show that as β in the adjustable texture increases (so decreasing perceived roughness), observers increase σ in it. The finding that observers could compensate for differences between surfaces in one parameter by adjusting the difference in the other parameter in a consistent way implies that both parameters influence a single percept of roughness. Fig. 2 also shows straight lines fitted to the five sets of points by least-squares regression. In all five cases, the correlation of β and log RMS height (σ) is significant (minimum value of $r = 0.860$, $df = 5$, $p < 0.05$).

3.3. Discussion

Experiment 1 shows that observers set consistent values of RMS height when matching the roughness of two surfaces. Note that this is not a trivial demonstration of an ability to match two surfaces for RMS height, because in this experiment observers were required to adjust RMS height in the one surface in order to compensate for a difference in roll-off factor β between it and the other surface. The regression lines plotted in Fig. 2 therefore pass through combinations of these two parameters which yield surfaces with the same perceived roughness. These *iso-roughness contours* are found to be close to linear in β–log RMS height space, with mean slope 1.12.

The results of Experiment 1 can be used to specify an estimator for perceived visual roughness in terms of the physical properties of a $1/f^{\beta}$ noise surface. The estimator that we propose consists of two stages: an isotropic, bandpass filtering of the surface height spectrum, followed by estimation of the variance of the filtered signal (note that the input to the filter is a surface height function; its relationship to image data is considered in Section 5). Perceived roughness r_{pu} can therefore be expressed in the frequency domain by:

$$r_{pu} = \int_0^{2\pi} \int_{f_1}^{f_2} |F(f)H(f)|^2 f \, \mathrm{d}f \, \mathrm{d}\theta \tag{2}$$

where $F(f)$ is the Fourier transform of the isotropic, bandpass filter; (f, θ) are the Fourier frequency co-ordinates in polar form, and f_1, f_2 are the lower and upper frequency bounds of the $1/f^{\beta}$ noise surface as specified previously. The subscript u denotes that, at this step, perceived roughness is unscaled, and measured only to an ordinal level. Because both the filter $F(f)$ and surface height spectrum $H(f)$ are isotropic, we can replace Eq. (2) with:

$$r_{pu} = 2\pi \int_{f_1}^{f_2} f|F(f)H(f)|^2 \, \mathrm{d}f \tag{3}$$

Since the surface height spectrum $H(f)$ is given by the parameters of the height map β and σ, it is now only necessary to define the

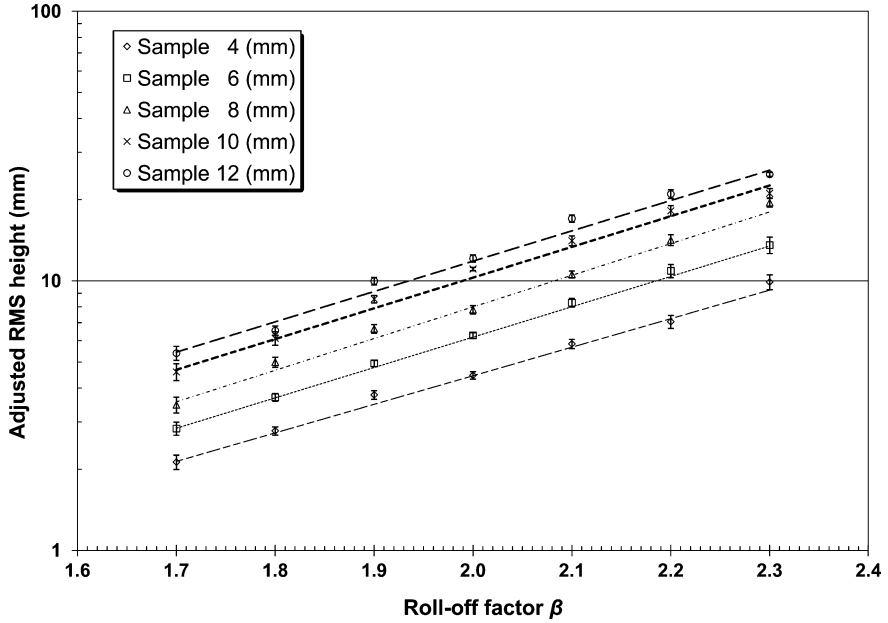

Fig. 2. Experiment 1: Mean RMS heights (plotted on a log scale) of adjustable surfaces with different β values, set by observers to match a sample surface. In the sample surface, β was always 2.0 and RMS height was one of five values. (Vertical bars) Standard errors of means across observers (SEM). (Broken lines) Best fit regression lines for each set of five points. From top to bottom, $r^2 = 0.841$, 0.830, 0.830, 0.788, and 0.740.

bandpass filter $F(f)$. We tested the fit to the data provided by bandpass filters of increasing complexity (square, ramp, and Gaussian; for details, see Padilla, 2008) and found the best fit with a Gaussian of log frequency:

$$F(f) = \frac{1}{\sigma_g\sqrt{2\pi}} \cdot e^{\frac{(\log(f) - \log(\mu))^2}{2\sigma_g^2}} \quad (4)$$

where σ_g and μ are parameters to be optimised. We can now calculate a predicted value for r_{pu} for any filter specified by (σ_g, μ) and any surface specified by (σ, β), by substituting Eqs. (1) and (4) into Eq. (3) and applying numerical integration to the result.

The parameters of the filter $[\mu, \sigma_g]$ must be fitted so that any two surfaces lying on an iso-roughness contour yield the same output and therefore the same unscaled perceived roughness. To find the values that give the best fit to the data from Experiment 1, an error value was calculated by taking the root mean square difference between predicted r_{pu} and the seven actual values of r_{pu} along each iso-roughness contour, normalising these to the same predicted r_{pu} value and then summing across the five contours. The minimum error is 0.0188 and lies at $\mu = 1.9821$ cycles/cm and $\sigma_g = 1.90$. With these values for its parameters, the estimator can then be used to calculate predicted iso-roughness contours in σ–β space under the conditions of Experiment 1.

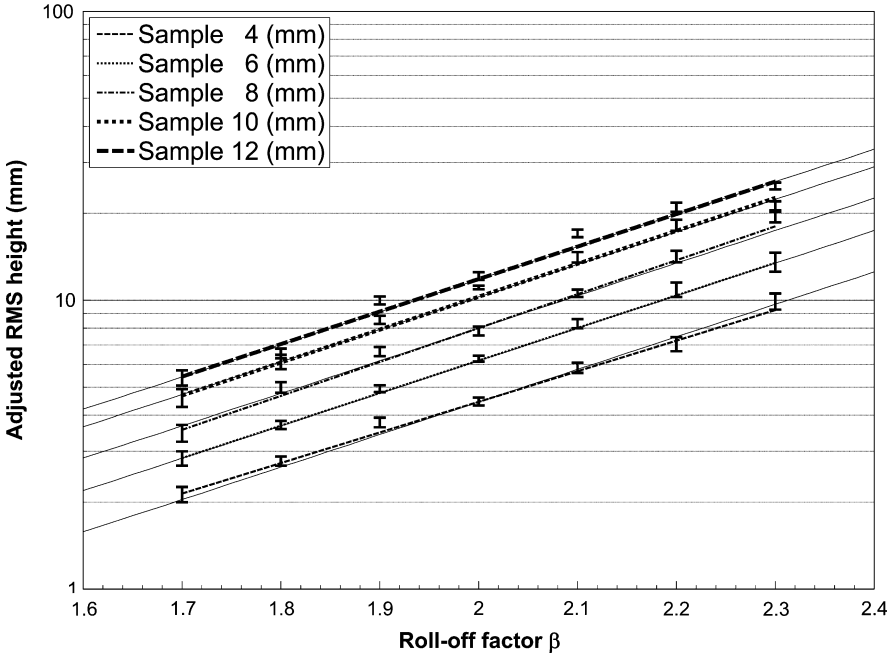

Fig. 3. Iso-roughness contours in β–σ space predicted by the Gaussian filter model for unscaled perceived roughness, compared to the data and best fit regression lines from Experiment 1. Regression lines are the solid grey lines extending beyond the range of experimental observations (i.e. below $\beta = 1.7$ and above $\beta = 2.3$).

Fig. 3 shows that the iso-roughness contours predicted by the estimator match those obtained in Experiment 1 closely. Additionally, from the forms of the estimator (Eq. (2)) and of the surface (Eq. (1)) it is clear that the model for r_{pu} is consistent with the basic observation that perceived roughness increases with RMS height σ (Padilla, 2008). These two facts therefore imply that the estimator can successfully measure perceived roughness to an ordinal level of measurement. Our next step is to construct a model that will take unscaled perceived roughness r_{pu} and convert it to a scaled measure. We use a bisection method (Fagot & Stewart, 1970) in Experiment 2 to do this, asking observers to adjust a surface texture until they perceive it to be midway between two sample textures in roughness. By repeating this procedure for different pairings of sample surfaces, we obtain data that can be used to fit a quadratic function for scaled perceived roughness r_{ps} in terms of estimator output r_{pu} to the data.

4. Experiment 2

4.1. Procedure

On each trial, observers were presented with three textured surfaces, two samples with fixed parameters and one adjustable texture. The two sample surfaces were presented in a single column on one monitor in portrait position, whilst the adjustable surface was presented on the second monitor; the centres of both monitor screens were equidistant from the observer. In the sample surfaces, β was always 2.0 and RMS heights were 4, 8, or 12 mm. On each trial, the two fixed samples had different RMS heights, and the three possible combinations occurred equally often. In the adjustable texture, β was 1.8, 1.9, 2.0, 2.1, or 2.2, and RMS height could be adjusted by the observer in the same way as in experiment one. Each of the 15 stimulus combinations was repeated three times, giving a total of 45 trials. The ten observers from experiment one took part, and were instructed to set the adjustable surface so that it appeared to be midway in roughness between the two samples, again imagining how the surfaces would feel if touched.

4.2. Results and discussion

Fig. 4 shows the RMS heights of the adjustable textures set by observers for different values of β in the three bisection tasks, plotted as iso-roughness contours in the same way as in Fig. 2. In all three cases, the correlation of β and log RMS height (σ) is significant (minimum value of $r = 0.896$, $df = 3$, $p < 0.05$), and values of r^2 are similar to those obtained in Experiment 1. The average slope of the three regression lines is 1.24, close to the slope of the iso-roughness contours obtained in Experiment 1, implying that performance in both the adjustment and the bisection tasks is determined by the same process.

The results of Experiment 2 also enable us to scale the model for perceived roughness derived from Experiment 1. Each bisection task provides five pairs of values of β and RMS height corresponding to a perceived roughness that is the average of the perceived roughnesses of the two samples. These 15 pairs of values are input to the filter-based estimator to obtain values of unscaled perceived roughness r_{pu}. With the addition of the estimator output values for the three sample surfaces, we next construct 18 quadratic expressions for scaled perceived roughness r_{ps} in terms of r_{pu}, with the form:

$$r_{ps} = ar_{pu}^2 + br_{pu} \tag{5}$$

Note that we assume that when the output of the filter-based estimator is zero, the perceived roughness of a surface is zero, and therefore there is no constant term in Eq. (5). Our method for deriving the coefficients a and b is described in full in Appendix. Briefly, assuming that the perceived roughness of the roughest of the three sample surfaces is 100, we have four unknowns; the coefficients a and b, and the values of r_{ps} for the other two sample surfaces. After multiplying values of r_{pu} by 10^{-8}, for convenience, the best fit quadratic to the 18 points, shown in Fig. 5, is:

$$r_{ps} = -7.04r_{pu}^2 + 52.6r_{pu} \tag{6}$$

Each set of five r_{pu} values obtained from a bisection task with the same sample pair, but with different β in the adjustable texture, corresponds to one value of r_{ps}. Although the values of r_{pu} within each of the three sets vary, they are significantly different from each other (one-way ANOVA: $F(2,12) = 103$; $p < 0.001$), indicating that the bisections made by observers are systematically related to the sample pairs. Eq. (6) provides a close fit to the data of Experiment 2 ($r^2 = 0.973$), and a better fit than a linear relationship ($r^2 = 0.902$). We therefore conclude that the model described by Eqs. (3), (4) and (6) provides a means of measuring, to an interval

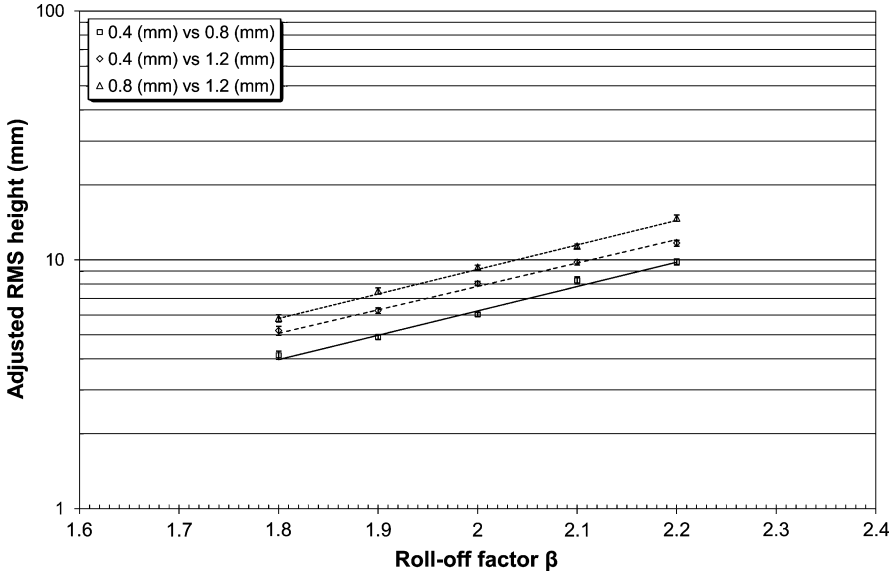

Fig. 4. Experiment 2: Mean RMS heights of adjustable surfaces with different β values, set by observers in the three bisection tasks. In the sample surfaces, β was always 2.0 and the pairs of RMS heights were as shown in the inset. Vertical bars: SEMs. From top to bottom, values of r^2 for the best fit regression lines are 0.822, 0.807, and 0.817.

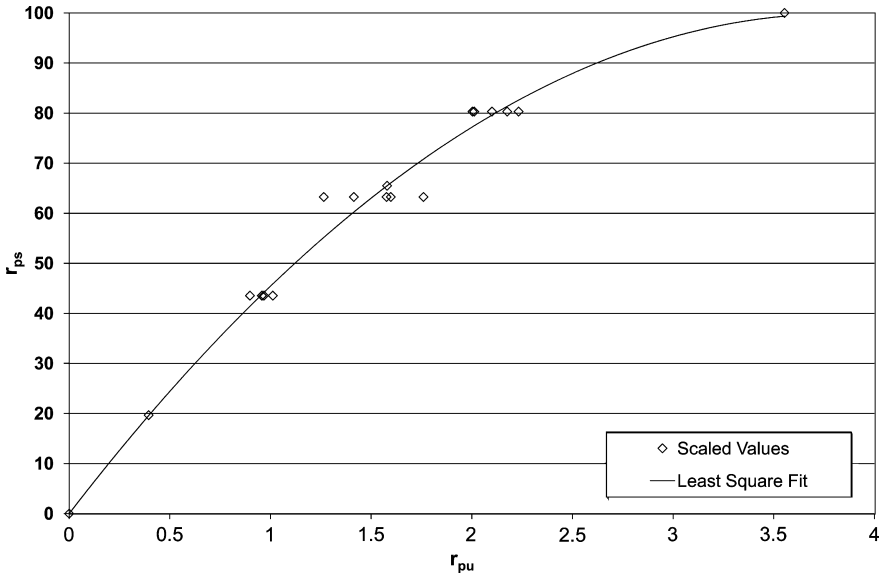

Fig. 5. Values of filter-based estimator output r_{pu} for each adjustable and sample surface in Experiment 2, plotted against values for perceived roughness r_{ps}, scaled using Eq. (6). The line is the least-squares fit using a quadratic model.

scale, the perceived roughness of isotropic, random-phase $1/f^{\beta}$ surfaces.

5. General discussion

The methodology for constructing and rendering synthetic surface textures used in these experiments is novel in several important respects. It allows the presentation of surfaces that are both realistic in appearance and have precisely specified physical properties, which can be adjusted in real time under an observer's control. It is possible to control independently the effects of illumination on a surface image, and to vary these in animations simulating in real time the effects of rotating a surface. Using these methods, it has been possible to specify precisely an estimator for the visually perceived surface roughness of isotropic, random-phase $1/f^{\beta}$ noise surfaces. This consists of two stages. First, unscaled perceived roughness is computed from the surface height spectrum, using a Gaussian filter with two fitted parameters (μ, σ_g), as described by Eqs. (3) and (4). Second, these values are scaled using Eq. (6), with two fitted coefficients (a, b).

5.1. How typical are $1/f^{\beta}$ noise surfaces of natural surfaces?

At present, the proposed estimator for perceived roughness applies only to random-phase, isotropic, $1/f^{\beta}$ noise surfaces. However, these are typical of the surface textures of a variety of naturally occurring materials. Scaling of the luminance power spectrum has been demonstrated by analyses of a wide variety of sets of images of natural scenes and surfaces (e.g. Field, 1987; Ruderman & Bialek, 1994; Tolhurst, Tadmor, & Chao, 1992; van der Schaaf & van Hateren, 1996). There is some variation between image sets, but they generally show scaling of the *image power* spectrum with roll-off factors in the range 1.7–2.2. In the stimuli that we have used, we found a realistic appearance where the roll-off factor of the *surface height magnitude* function fell between 1.7 and 2.3. Two points need to be taken into account in comparing these figures.

First, what is the relationship between the height magnitude spectrum of a surface and the luminance magnitude spectrum of its image when it is illuminated? Assuming a linearised Lambertian model of reflectance (i.e. a surface with low slope angles), and no effect of shadows and interreflections, Chantler, Petrou, Penirsche, Schmidt, and McGunnigle (2005) show that the image and height magnitude spectra $I(f,\theta)$ and $H(f,\theta)$ are related by:

$$I(f,\theta) = -\mathrm{i}f\cos(\theta - \alpha)\cos(\varepsilon)H(f,\theta) \tag{7}$$

where α and ε are the azimuth and elevation of a point illumination source. It follows from Eq. (7) that

$$\beta_i = \beta_h - 1 \tag{8}$$

where β_i and β_h are the roll-off factors of the image luminance magnitude spectrum and the surface height magnitude spectrum, respectively (note that β_h is the same variable that we have so far denoted simply as β, for convenience). The assumptions underlying this model are realistic for a number of natural textured surfaces, and for synthetic surfaces of the kind used here, as Chantler (1995) showed that the model closely predicted measurements of the effect of illumination angle on the image spectrum.

Following Eq. (8), a surface with $\beta_h = 2$ will give rise to an image with β_i approximately equal to 1. However, this is the roll-off factor of the luminance *magnitude* spectrum, and must be doubled to give that of the *power* spectrum, the parameter used in the literature on scaling of natural images. Overall, if one of the surfaces used in our experiments has a value of two for its height magnitude function (β_h), then its rendered image will have a value of β for its luminance power spectrum of approximately 2. We conclude that there is a close correspondence between the properties of the synthetic surfaces that we used and those of naturally occurring surfaces and scenes.

5.2. Implementation in the visual system

The estimator that we propose has the mathematical form of a filter-rectify-filter (or linear-nonlinear-linear) model commonly used in models of texture segregation (e.g. Bergen & Landy, 1991). The input is passed through a linear spatial filter, the variance of the resulting signal is obtained by a squaring operation, and the result is then summed over the whole surface. However, the algorithm is being applied here in a different context from texture segregation. In particular, its input is not image luminance signals, but surface height data. If it is implemented in the visual system as a distinct process, it must therefore follow stages in

which surface relief is recovered from the image. In the displays that we used, this must be achieved using shading information, together with changes in shading as the rendered surface rotates relative to the light source. In natural circumstances, binocular disparity, motion parallax and other depth cues would also come into play. Perception of surface roughness will therefore depend both on processes involved in the recovery of surface depth and on those implementing our proposed estimator, and so any bias in the first stage will affect the perceived roughness of a surface.

6. Conclusions

We have derived a model for measuring on a ratio scale the visually perceived roughness of synthetic surfaces generated by a $1/f^{\beta}$ noise process. This is the first time that it has been possible to specify an estimator which measures a perceived dimension of texture, given a physical description of its surface. Because the model is based on experiments using $1/f^{\beta}$ noise surfaces, it can be applied to a large class of natural materials, and there is scope in future work to extend it to other classes of surfaces with directionally oriented or regular textures.

Appendix A. Derivation of scaling parameters (Experiment 2)

The data from Experiment 2 were used to determine suitable values for the parameters for the scaling relationship (Eq. (5)). This appendix describes this estimation process.

Section 4.1 described how ten observers carried out trials in which they adjusted the RMS height (σ) of a surface until it was perceived to be midway in roughness between two reference surfaces. Three different types of reference surface were used:

Surface type *d*: $\beta = 2, \sigma = 4$ mm
Surface type *e*: $\beta = 2, \sigma = 8$ mm
Surface type *f*: $\beta = 2, \sigma = 12$ mm

Individual reference surfaces of the same *type* differed only by phase spectra. When visually inspected all surfaces used did not appear to contain any distinct phase alignments and were therefore likely to be of the same perceived roughness.

Each observer performed fifteen trials using adjustable surfaces of five different β (1.8, 1.9, 2.0, 2.1, & 2.2) with three different reference pair types: (*d*,*e*), (*e*,*f*) and (*d*,*f*). Thus they produced five new surfaces with a perceived roughness of $(d_{ps} + e_{ps})/2$, five of $(e_{ps} + f_{ps})/2$ and five of $(d_{ps} + f_{ps})/2$. For each observer we calculated the unscaled roughness (r_{pu}) of each of their fifteen new surfaces from the (β, σ) values. The median values were then taken across observers to provide fifteen estimates of r_{pu} (five for each reference pair type). Including the data from the three reference pair types provides eighteen corresponding values of (r_{ps}, r_{pu}):

r_{ps}:	d_{ps}	e_{ps}	f_{ps}	$(d_{ps} + e_{ps})/2$	$(e_{ps} + f_{ps})/2$	$(d_{ps} + f_{ps})/2$
r_{pu}:	1 value	1 value	1 value	5 values	5 values	5 values

When these data are substituted into Eq. (5) this provides a set of 18 homogeneous equations with five unknowns (*a*, *b*, d_{ps}, e_{ps}, and f_{ps}).

However, we define our roughest reference surface to have a perceived roughness $f_{ps} = 100$, leaving four unknowns. We solve the resulting set of over-constrained simultaneous equations using least-squares to provide estimates of −7.04 and 52.6 for *a* and *b*, respectively.

References

Amadasun, M., & King, R. (1989). Textural features corresponding to textural properties. *IEEE Transactions on Systems, Man, and Cybernetics, 19*, 1264–1274.

Balas, B. J. (2006). Texture synthesis and perception: Using computational models to study texture representations in the human visual system. *Vision Research, 46*, 299–309.

Belhumeur, P. N., Kriegman, D. J., & Yuille, A. L. (1999). The bas-relief ambiguity. *International Journal of Computer Vision, 35*, 33–44.

Bergen, J. R., & Landy, M. S. (1991). Computational modelling of visual texture segregation. In M. S. Landy & J. A. Movshon (Eds.), *Computational models of visual processing* (pp. 253–271). Cambridge, MA: MIT Press.

Blume, H., Steven, P., Ho, A., Stevens, F., Abileah, A., Robinson, S., et al. (2003). Characterization of liquid-crystal displays for medical images: II. medical imaging 2003: Visualization, image-guided procedures, and display. *Proceedings of the SPIE, 5029*, 449–473.

Brodatz, P. (1966). *Textures: A photographic album for artists and designers*. New York: Dover Publications.

Campbell, F. W., & Robson, J. G. (1968). Application of Fourier analysis to the visibility of gratings. *Journal of Physiology, 197*, 551–566.

Chantler, M. J. (1995). Why illuminant direction is fundamental to texture analysis. *IEE Proceedings: Vision Signal and Image Processing, 142*, 199–206.

Chantler, M., Petrou, M., Penirsche, A., Schmidt, M., & McGunnigle, G. (2005). Classifying surface texture while simultaneously estimating illumination direction. *International Journal of Computer Vision, 62*, 83–96.

Cook, R. L. (1984). Shade trees. In *Proceedings of the 11th annual conference on computer graphics and interactive techniques (pp. 223–231). New York, NY: ACM/SIGGRAPH.*

Fagot, R. F., & Stewart, M. R. (1970). Test of a response bias model of perception. *Perception and Psychophysics, 7*, 257–262.

Field, D. J. (1987). Relations between the statistics of natural images and the response properties of cortical cells. *Journal of the Optical Society of America A, 4*, 2379–2394.

Harvey, L. O., & Gervais, M. J. (1981). Internal representation of visual texture as the basis for the judgement of similarity. *Journal of Experimental Psychology: Human Perception and Performance, 7*, 741–753.

Heaps, C., & Handel, S. (1999). Similarity and features of natural textures. *Journal of Experimental Psychology: Human Perception and Performance, 25*, 299–320.

Ho, Y. X., Landy, M. S., & Maloney, L. T. (2006). How direction of illumination affects visually perceived surface roughness. *Journal of Vision, 6*, 634–648.

Ho, Y. X., Maloney, L. T., & Landy, M. S. (2007). The effect of viewpoint on perceived visual roughness. *Journal of Vision, 7*, 1–16.

Koenderink, J. J., van Doorn, A. J., Kappers, A. M. L., te Pas, S. F., & Pont, S. C. (2003). Illumination direction from texture shading. *Journal of the Optical Society of America A, 20*, 987–995.

Long, H., & Leow, W. K. (2001). Perceptual texture space improves perceptual consistency of computational features. IJCAI 2001, August 4th–10th, Seattle, pp. 1391–1396.

Malik, J., & Rosenholtz, R. (1997). Computing local surface orientation and shape from texture for curved surfaces. *International Journal of Computer Vision, 23*, 149–168.

Mandelbrot, B. B. (1983). *The fractal geometry of nature*. New York: W.H. Freeman.

Padilla, S. (2008) *Mathematical models for perceived roughness of three-dimensional surface textures*. Ph.D. thesis, Heriot-Watt University.

Portilla, J., & Simoncelli, E. P. (2000). A parametric texture model based on joint statistics of complex wavelet coefficients. *International Journal of Computer Vision, 40*, 49–71.

Rao, A. R., & Lohse, G. L. (1996). Towards a texture naming system: Identifying relevant dimensions of texture. *Vision Research, 36*, 1649–1669.

Ruderman, D. L., & Bialek, W. (1994). Statistics of natural images: Scaling in the woods. *Physical Review Letters, 73*, 814–817.

Saunders, J. A., & Backus, B. T. (2006). Perception of surface slant from oriented textures. *Journal of Vision, 6*, 882–897.

Saupe, D. (1988). Algorithms for random fractals. In H. O. Peitgen & D. Saupe (Eds.), *The science of fractal images* (pp. 71–113). Berlin: Springer Verlag.

Tamura, H., & Mori, S. & Yamawaki, T. (1978). Textural features corresponding to visual perception. *IEEE Transactions on Systems, Man, and Cybernetics, 8*, 460–473.

Tolhurst, D. J. , Tadmor, Y. , & Chao, T. (1992). Amplitude spectra of natural images. *Ophthalmic and Physiological Optics, 12*, 229–232.

van der Schaaf, A. & van Hateren, J. H. (1996). Modelling the power spectra of natural images: Statistics and information. *Vision Research, 28*, 2759–2770.